Articles

Inhibition of Membrane-Type 1 Matrix Metalloproteinase by Hydroxamate Inhibitors: An Examination of the Subsite Pocket

Minoru Yamamoto,[†] Hideki Tsujishita,[†] Noriyuki Hori,[†] Yuichi Ohishi,[‡] Shintaro Inoue,[‡] Shoji Ikeda,*[,†] and Yasunori Okada*[,§]

New Drug Discovery Research Laboratory, Kanebo Ltd., 1-5-90 Tomobuchi-Cho, Miyakojima-Ku, Osaka 534, Japan, Basic Science Laboratory, Kanebo Ltd., 5-3-28 Kotobuki-Cho, Odawara, Kanagawa 250, Japan, and Department of Molecular Immunology and Pathology, Cancer Research Institute, Kanazawa University, 13-1 Takara-machi, Kanazawa, Ishikawa 920, Japan

Received June 18, 1997

The membrane-type 1 matrix metalloproteinase (MT1-MMP) has been reported to mediate the activation of pro-gelatinase A (proMMP-2), which is associated with tumor proliferation and metastasis. MT1-MMP can also digest extracellular matrix (ECM) such as interstitial collagens, gelatin, and proteoglycan and thus may play an important role in pathophysiological digestion of ECM. We studied the inhibitory effect of various hydroxamate MMP inhibitors, including known inhibitors such as BB-94, BB-2516, GM6001, and Ro31-9790, on a deletion mutant of MT1-MMP lacking the transmembrane domain (ΔMT1) to further characterize the enzyme and develop a selective inhibitor for MT1-MMP. The evaluation of the inhibitory activities of various hydroxamates reveals general structural profiles affecting selectivities toward MMPs. In particular, a longer side chain at the P1′ position is preferable for the binding to MMP-2, -3, and -9 and MT1-MMP. For the P2′ position, an α-branched alkyl group is critical for the binding toward ΔMT1, while the introduction of a bulky group at the α-position of hydroxamic acid seems to diminish the activity against ΔMT1. Summation of the data on the sensitivity of ΔMT1 to various hydroxamate inhibitors indicates that (1) the volume of the S1′ subsite of ΔMT1 is similar to that of MMP-2, -3, and -9, which is bigger than that of MMP-1, and (2) the S1 and S2′ subsites are narrower than those in other MMPs. On the basis of these results, the hydroxamates with a P1′ phenylpropyl and P2′ α-branched alkyl group were synthesized and evaluated for inhibitory activity. These inhibitors (**1h**,**i**) showed strong activity against ΔMT1 over MMP-1, but no selectivity between ΔMT1 and MMP-9. These results are explained using molecular modeling studies conducted on MT1-MMP.

Introduction

The matrix metalloproteinases (MMPs) are a family of zinc endopeptidases that degrade the major extracellular matrix (ECM) macromolecules under both physiological and pathological conditions.[1] The overexpression and activation of MMPs have been involved in a range of diseases. For example, gelatinase A (MMP-2) is reported to be associated with invasion and metastasis in various human cancers.[2] In general MMPs are secreted as inactive zymogens (proMMPs) and are activated through an initial cleavage by the action of proteinases (trypsin, plasmin, chymotrypsin, neutrophil elastase, and plasma kallikrein) and the subsequent autolytic cleavage of the pro-peptide.[3] However, proMMP-2 has no sequence that is susceptible to proteolytic activation by these serine proteinases. Consequently, the mechanism of proMMP-2 activation has attracted considerable attention. Extensive research on the activation mechanism of proMMP-2 has resulted in the recent discovery of a membrane-type 1 MMP (MT1-MMP) as an activator of proMMP-2.[4] The expression of MT1-MMP in human stomach and breast carcinomas is reported to correlate well with the activation of proMMP-2 which is mediated by MT1-MMP.[5] Furthermore, since the structure of the catalytic domain of MT1-MMP is similar to that of other MMPs, one might expect similar enzymatic activity of MT1-MMP to ECM macromolecules. In fact, Ohuchi et al.[6] have recently demonstrated that both a deletion mutant of MT1-MMP lacking the transmembrane domain (ΔMT1) and a secreted form of native MT1-MMP digest fibrillar collagens like MMP-1 as well as gelatin, proteoglycan, fibronectin, vitronectin, and laminin-1. These findings suggest that MT1-MMP plays a dual role in the pathophysiological digestion of ECM through the activation of proMMP-2 and direct cleavage of ECM. Because of the critical role that MT1-MMP plays in cancer invasion and metastasis, the inhibition of the enzyme is an important therapeutic target for cancer chemotherapy. In addition, a selective inhibitor of MT1-MMP would be a desirable element for studies aimed at delineating the physiological roles of MT1-MMP. Yet, no reports

[†] New Drug Discovery Research Laboratory, Kanebo Ltd.
[‡] Basic Science Laboratory, Kanebo Ltd.
[§] Kanazawa University.

S0022-2623(97)00404-4 CCC: $15.00
Published on Web 03/21/1998

Scheme 1. Synthesis of Hydroxamate Inhibitors with No α-Substituent[a]

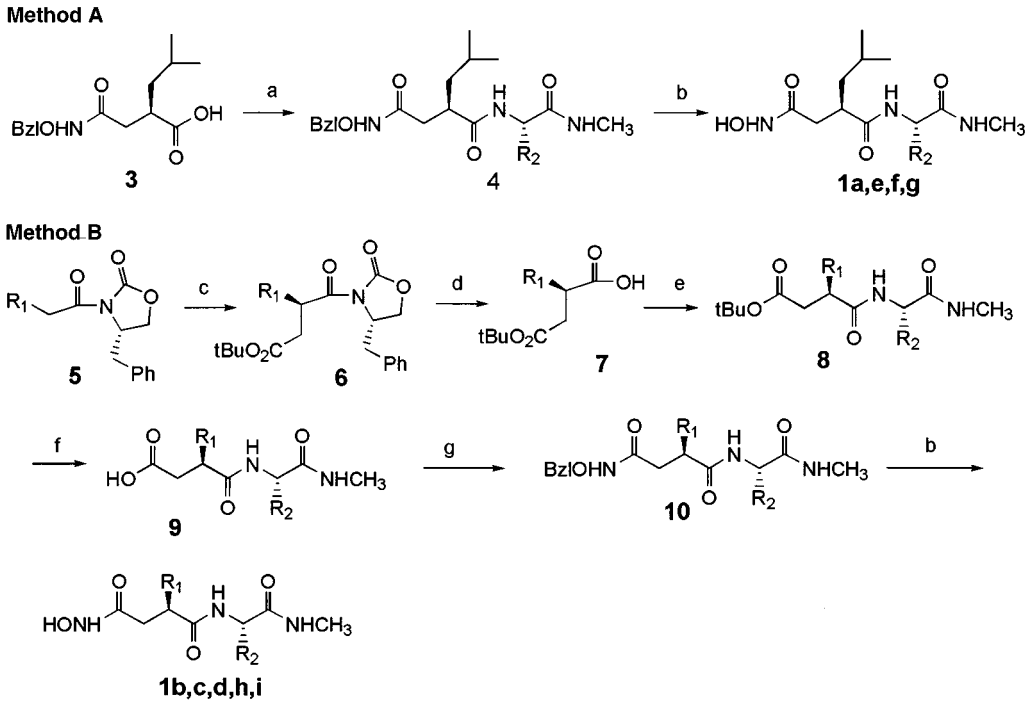

[a] Reagents and conditions: (a) $H_2NCHR_2CONHCH_3$, WSC, DMF; (b) H_2, 10% Pd/C, MeOH; (c) $(Me_2CH)_2NH$, *n*-BuLi, *t*-butyl bromoacetate, THF; (d) aq H_2O_2, LiOH; (e) $H_2NCHR_2CONHCH_3$, HOBT, WSC, DMF; (f) TFA; (g) H_2NOBzl, HOBT, WSC, DMF. WSC: 1-[3-(dimethylamino)propyl]-3-ethylcarbodiimide hydrochloride.

on structure−activity relationships of hydroxamate inhibitors against MT1-MMP are available.

In the present paper, we have investigated the structure−activity relationship of various hydroxamate inhibitors, including known inhibitors such as BB-94 (**2d**),[22] BB-2516 (**2c**),[21] GM6001 (**1g**),[20] and Ro31-9790 (**1f**),[23] against ΔMT1 to better understand the nature of this enzyme and obtain information for the design of superior inhibitors.

Chemistry

The P1′ isobutyl hydroxamates (**1a**,**e**,**f**) with no substituent at the 3-position of succinic acid (α-position) were synthesized from 4-[*N*-(benzyloxy)amino]-(2*R*)-isobutylsuccinic acid (**3**)[7] as shown in Scheme 1, method A. Other hydroxamates (**1b**−**d**,**h**,**i**) with no substituent at the α-position were prepared from 4-(*tert*-butyloxy)-(2*R*)-substituted succinic acid **7** by method B as shown in Scheme 1.

The hydroxamates (**2**) with a substituent at the α-position were prepared from *tert*-butyl 4-methyl-(2*S*)-bromopentanoate (**10**) by the method outlined in Scheme 2, method C. P2′ (tetrahydronaphthyl)methyl derivative **2e** was obtained by hydrogenation of the P2′ naphthylmethyl derivative **16e** with 10% Pd/C in acetic acid (Scheme 2). It should be noted that this reduction did not occur in methanol with 10% Pd/C.

BB-94[22] and BB-2516[21] were obtained using methods described in previous patents. GM6001 and Ro31-9790 were synthesized using method A, Scheme 1.

Results and Discussion

The inhibitory effects of various hydroxamate inhibitors were determined against human ΔMT1, MMP-1, MMP-2, MMP-3, and MMP-9. Their inhibitory activities are shown in Table 1. Recent X-ray crystallographic studies showed that the S1′ subsite in MMP is the most well-defined area of binding and consists of a hydrophobic pocket which varies in depth for the different MMPs.[8] These results suggest that the selectivity of peptidomimetic hydroxamates varies depending on the P1′ substituent.[9] Therefore, we examined the effect of the P1′ substituent on the inhibition of ΔMT1. First, a P2′ substituent was fixed to the phenyl group, because our previous studies showed that hydroxamates with a phenyl group at the P2′ substituent can possess good oral activity.[7] The P1′ isobutyl derivative **1a** exhibited an IC_{50} value of 10^{-8} M against ΔMT1. A similar value was found against MMP-1, -2, and -9. The modification of the P1′ isobutyl group (**1a**) to a phenylethyl group (**1b**) decreased the inhibitory activity against ΔMT1 with a concomitant decrease in that against MMP-1. The elongation of the P1′ substituent from phenylethyl (**1b**) to phenylpropyl (**1c**) led to a 10-fold increase in inhibition against ΔMT1. This substitution also increased the inhibitory activities against MMP-2, -3, and -9 except for MMP-1. The P1′ nonyl derivative **1d** showed poorer inhibitory activity against ΔMT1 than the phenylpropyl derivative **1c** but exhibited a strong increase in activity against gelatinases (MMP-2 and -9). These structure−activity studies on the P1′ substituent suggest that the volume of the S1′ subsite of ΔMT1 is similar to that of MMP-3, which is larger than that of MMP-1 yet smaller than those of MMP-2 and -9.

We next examined the effect of the P2′ substituent on the inhibitory activity of ΔMT1. Modification of the P2′ substituent from a phenyl group (**1a**) to a cyclohexyl group (**1e**) or *tert*-butyl group (**1f**, Ro31-9790) improved the inhibitory activity against ΔMT1 by a factor of about 10. However, the P2′ indolylmethyl derivative **1g**

Scheme 2. Synthesis of Hydroxamate Inhibitors with α-Substituent (R_3)[a]

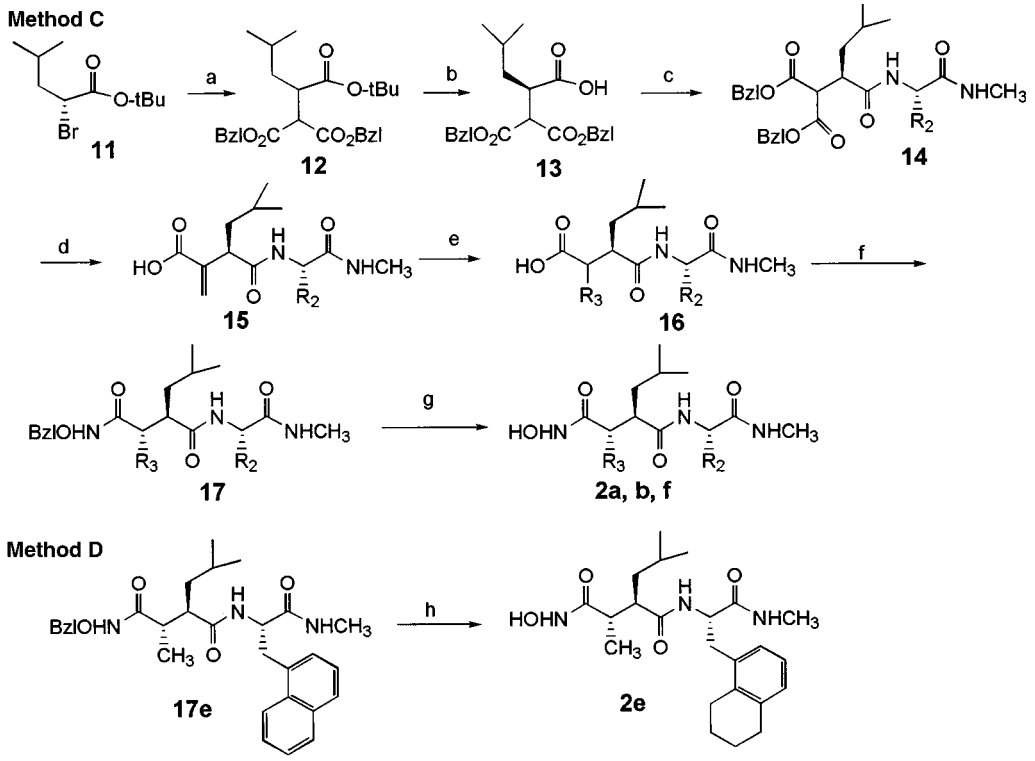

[a] Reagents and conditions: (a) dibenzyl malonate, *t*-BuOK; (b) TFA; (c) $H_2NCHR_2CONHCH_3$, HOBT, WSC, DMF; (d) i. H_2, 10% Pd/C, MeOH, ii. HCHO, piperidine; (e) morpholine or H_2, 10% Pd/C; (f) H_2NOBzl, HOBT, WSC, DMF; (g) H_2, 10% Pd/C, MeOH; (h) H_2, 10% Pd/C, AcOH. WSC: 1-[3-(dimethylamino)propyl]-3-ethylcarbodiimide hydrochloride.

Table 1. In Vitro Inhibitory Activities against ΔMT1 and Other MMPs

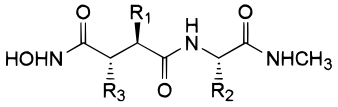

compd	R_1	R_2	R_3	IC_{50} (nM) ΔMT1	MMP-1	MMP-2	MMP-3	MMP-9
1a	$-CH_2CH(CH_3)_2$	$-C_6H_5$	H	19.3	15	42.5	4.4	14
1b	$-(CH_2)_2C_6H_5$	$-C_6H_5$	H	105	92	46.3	17	11
1c	$-(CH_2)_3C_6H_5$	$-C_6H_5$	H	8.5	89	3.2	9.6	3.3
1d	$-(CH_2)_8CH_3$	$-C_6H_5$	H	17.6	90	1.6	100	0.2
1e	$-CH_2CH(CH_3)_2$	$-C_6H_{11}$	H	2.3	5.4	8.4	2.3	5
1f (Ro31-9790)	$-CH_2CH(CH_3)_2$	$-C(CH_3)_3$	H	1.9	3	7.4	NT[b]	12
1g (GM6001)	$-CH_2CH(CH_3)_2$	A[a]	H	13.4	1.5	1.1	1.9	0.5
2a	$-CH_2CH(CH_3)_2$	$-C_6H_5$	CH_3	56	3	7.5	1.9	3.9
2b	$-CH_2CH(CH_3)_2$	$-C_6H_5$	B[a]	72	3.5	NT[b]	61	45
2c (BB-2516)	$-CH_2CH(CH_3)_2$	$-C(CH_3)_3$	OH	1.82	2	5.1	4.4	8
2d (BB-94)	$-CH_2CH(CH_3)_2$	$-CH_2C_6H_5$	C[a]	3	0.4	1	0.65	0.2
2e	$-CH_2CH(CH_3)_2$	D[a]	CH_3	2.08	0.3	0.3	0.6	0.3

[a] A, (indol-3-yl)methyl; B, (4-morpholino)methyl; C, 2-thienylthiomethyl; D, (5,6,7,8-tetrahydro-1-naphthyl)methyl. [b] Not tested.

(GM6001) showed almost the same inhibitory activity against ΔMT1 as the P2′ phenyl derivative **1a**, although **1g** was more potent against other MMPs. Thus, the α-branched alkyl group as a P2′ substituent should be favorable for the inhibition of ΔMT1. MT1-MMP has been reported to cleave the Asn37−Leu38 peptide bond of the proMMP-2 amino acid sequence Ser35-Cys36-Asn37-Leu38-Phe39-Val40,[10] suggesting that the Phe39 corresponds to the S2′ subsite. The orientation of phenyl group of compound **1a** appears to differ from that of the benzyl group of Phe39. We suggest that **1a** does not efficiently interact with the active site because of this difference in orientation of the P2′ substituent. The modification of the phenyl group (**1a**) to a cyclohexyl group (**1e**) seems to change the orientation of the P2′ substituent similar to that of a benzyl group and thus leads to an improvement in activity. It is interesting to note that P2′ phenyl derivative **1a** showed weaker activity toward MT1-MMP than the P2′ cyclohexyl (**1e**) and *tert*-butyl (**1g**, Ro31-9790) derivatives, though the difference between these compounds is rather small. This would imply that the S2′ subsite of MT1-MMP is better defined than those in other MMPs, and MT1-MMP strongly recognizes the shape of the P2′ substituent.

It has been reported that the introduction of a substituent at the α-position of hydroxamic acids generally enhances inhibitory activity.[11] However, the introduction of a methyl (**2a**) or morpholinomethyl (**2b**) group into the α-position of **1a** and the introduction of

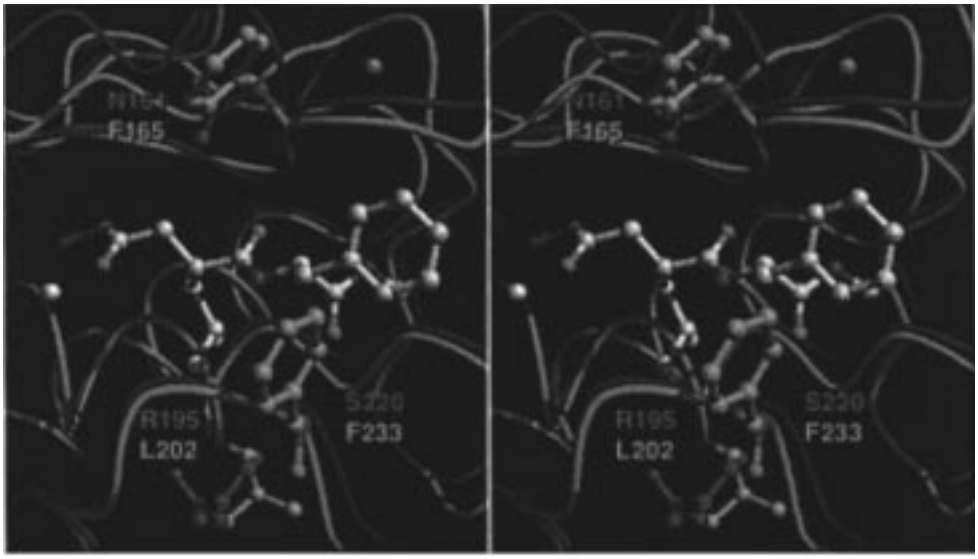

Figure 1. Stereorepresentation of the modeled active site of MT1-MMP1. The active site of the crystal structure of MMP-1,[18] complexed with an inhibitor ([4-(*N*-hydroxyamino)-2(*R*)-isobutylsuccinyl]-L-phenylalanine-*N*-methylamide) as described in the literature, is also shown. The main chains of both enzymes are represented by tubes and are colored dark blue (MT1-MMP) and light blue (MMP-1), respectively. Only the side chains of the amino acids that contribute to the ligand specificity (see text) are shown, and they are colored orange (MT1-MMP) and green (MMP-1), respectively. The inhibitor is colored yellow. White and magenta spheres represent the catalytic zinc ion and the calcium ion, respectively.

Table 2. In Vitro Inhibitory Activities against ΔMT1, MMP-1, and MMP-9

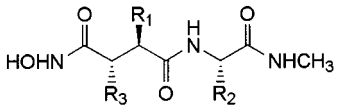

				IC_{50} (nM)		
compd	R_1	R_2	R_3	ΔMT1	MMP-1	MMP-9
1h	$-(CH_2)_3C_6H_5$	$-C(CH_3)_3$	H	1.9	21	1.3
1t	$-(CH_2)_3C_6H_5$	$-CH(CH_3)_2$	H	2.5	93	2.8
2f	$-CH_2CH(CH_3)_2$	$-C_6H_{11}$	CH_3	13	2.9	0.9

a hydroxyl group (**2c**, BB-2516) in that of **1f** (Ro31-9790) have not improved the inhibitory activity against ΔMT1. In the case of **2a**,**b**, the introduction of an α-substituent decreased the inhibitory activity of ΔMT1 as compared with a non-α-substituted derivative (**1a**). These results suggest that the S1 subsite of MT1-MMP is quite tight.

Potent inhibitory activity against ΔMT1 was seen with broad-spectrum inhibitors against various MMPs, including compounds **2d** (BB-94) and **2e**. Both of these compounds have a thienylthiomethyl and a methyl group at the α-position of hydroxamic acid, respectively. However, inhibition against ΔMT1 was less than that seen with other MMPs such as MMP-1, -2, -3, and -9. Therefore, it seems likely that the α-substituent does not enhance the inhibitory activity of ΔMT1.

On the basis of the above structure−activity studies, the hydroxamates with a P1′ phenylpropyl and P2′ α-branched alkyl group (i.e., *tert*-butyl and isopropyl) were synthesized so as to develop more selective inhibitors for ΔMT1. The modification of the P2′ phenyl group in compound **2a** to a cyclohexyl group was also carried out in order to confirm the above hypothesis. The inhibition seen with these compounds against ΔMT1 and MMP-1 and -9 is shown in Table 2. Compounds **1h**,**i** exhibited potent activity against ΔMT1 and MMP-9. As hoped the inhibition of ΔMT1 using **2f** was improved more than 4-fold compared with **2b**. Compounds **1h**,**i** are selective inhibitors of ΔMT1 when compared to MMP-1, but there is no selectivity between ΔMT1 and MMP-9.

	S1 site	S1′ site	S2′ site
MMP-1	159 GG**N**LAHAF 166	193 LH**R**VAAHE 200	215 ALMYP**S**Y 221
MMP-2	159 DG**L**LAHAF 166	368 LF**L**VAAHE 375	390 ALMAP**I**Y 396
MMP-3	161 GN**V**LAHAY 168	195 LF**L**VAAHE 202	217 ALMYP**L**Y 223
MMP-9	166 DG**L**LAHAF 173	376 LF**L**VAAHE 383	398 ALMYP**M**Y 404
MT-MMP-1	163 GG**F**LAHAY 170	200 LF**L**VAAHE 207	228 AIMAP**F**Y 234

Figure 2. Comparison of amino acid sequences of MMPs. Bold letters indicate the amino acids that contribute to the ligand specificity (see text and Figure 1). The sequence alignment was taken from ref 30.

To elucidate structural factors that determine the selectivity, we constructed a structural model of the catalytic domain of MT1-MMP using the Swiss-Model Protein Modeling Server.[12,13] This server automatically builds a three-dimensional model of a given sequence based on the sequence similarity with related proteins whose three-dimensional structures are known. The model of MT1-MMP was constructed from the crystal structures of human neutrophil collagenase (MMP-8) (Protein Data Bank: 1MNC,[14] 1JAO,[15] and 1JAP[16]), matrilysin (MMP-7) (1MMR and 1MMP[17]), and MMP-1 (1HFC[18] and 1CGE[19]).

Figure 1 compares the MT1-MMP model with fibroblast collagenase (MMP-1). As shown in this figure, clearly one can see that the whole structure of MT1-MMP is very similar to that of MMP-1. However, upon close examination of the model, we see two characteristic phenylalanines (Phe233 and Phe165) that could contribute to the ligand selectivity of MT1-MMP. These residues are part of the S1 and S2′ subsites in the enzyme. In the cases of other MMPs, these phenylalanines are replaced by smaller amino acid residues (see Figure 2). Taken together we conclude that the S1 and S2′ subsites in MT1-MMP are much narrower than those in other MMPs. Especially, Phe165 is close to the

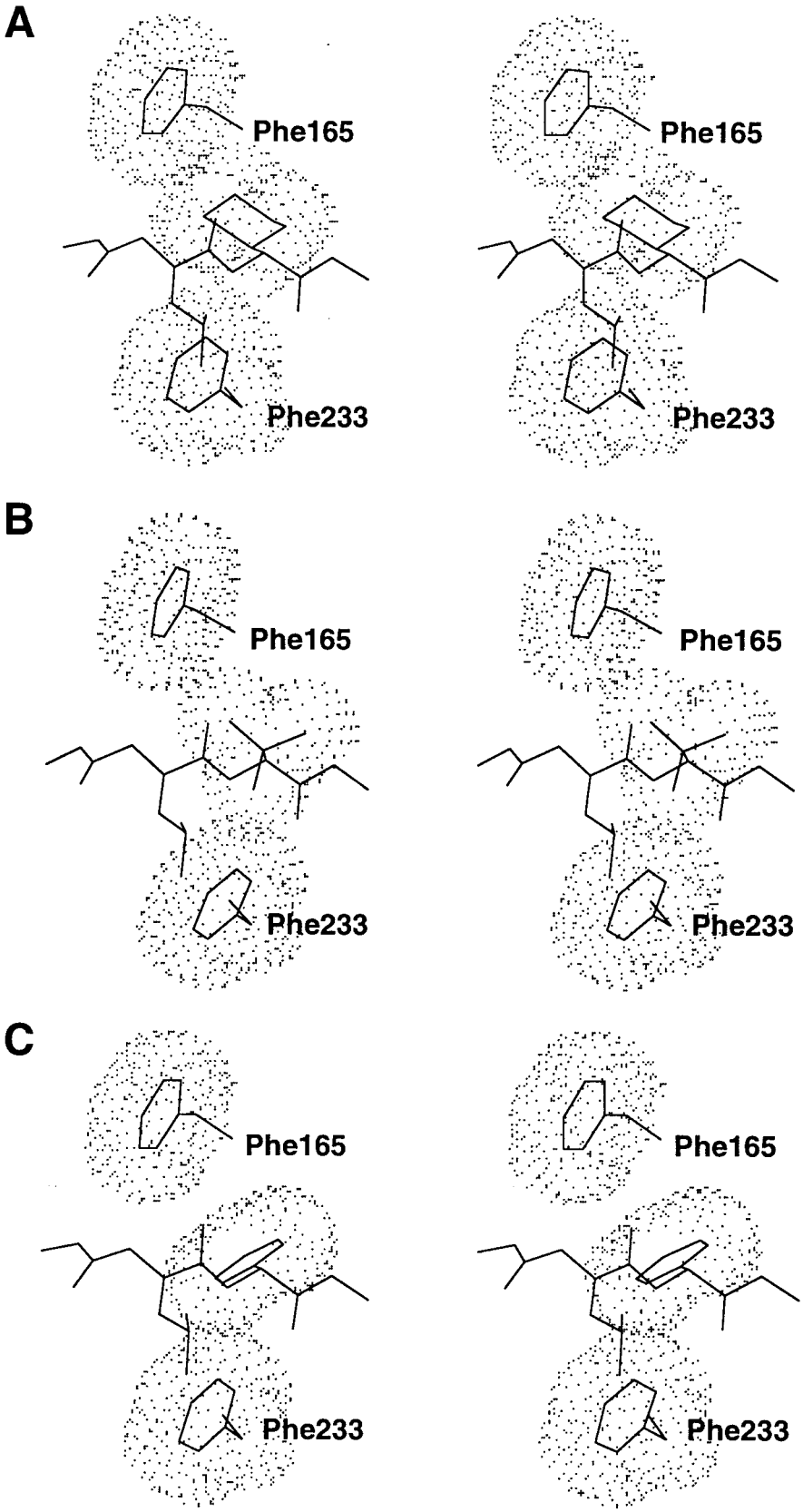

Figure 3. Stereorepresentation of the models of the complexes of MT1-MMP and (A) compound **1e**, (B) compound **1f**, (C) compound **1a**. Only the inhibitors and the side chains of Phe165 and Phe233 are shown for clarity. Dotted surfaces represent the vdW volumes of the side chains of Phe165 and Phe233 and the P2′ substituents of the inhibitors.

α-position of hydroxamic acid of the inhibitors (P1 position). As mentioned above, a bulky moiety at this position seemed to reduce the inhibitory activity toward MT1-MMP. This might be because such a bulky side chain would cause steric crash with Phe165 in MT1-MMP.

For a detailed investigation of the S2′ subsite, we constructed structural models of the complex with several inhibitors (**1a**,**e**,**f**). Initially we superposed the MT1-MMP model on the crystal structure of MMP-1 (Figure 1) and then aligned the target inhibitors on the ligand observed in the MMP-1 crystal structure. Next we performed energy minimization on these model complexes. Our constructed models and all calculations were done by SYBYL 6.3 (Tripos Inc., St. Louis, MO). During the minimization process all inhibitors and Phe165/Phe233, both believed to be an important part of the S2′ subsite, were allowed to move. Electrostatic interactions were calculated with a distance-dependent dielectric constant of 1, for the implicit treatment of the solvent effect. Atomic charges were calculated by the Gasteiger−Hückel method built into SYBYL. The minimizations were terminated when rms of the gradients potential energy was below 0.05 kcal/(mol Å).

Figure 3 shows the various modeled complexes we obtained. Among the targeted inhibitors, compound **1a** having a phenyl group at its P2′ position exhibited rather modest activity against MT1-MMP when compared with **1e** or **1f**, which have a cyclohexyl or *tert*-butyl group in this position, respectively. Interestingly, the P2′ substituents of these three compounds all fit very well in the S2′ subsite as defined by Phe165 and Phe233 (Figure 3). In the case of the bulky *tert*-butyl group (**1f**), the side chain of Phe233 shifted slightly allowing the *tert*-butyl group to bind into the subsite properly (Figure 3B). The only difference in these models was the value of the χ_1 dihedral angle (defined by $N-C_\alpha-C_\beta-C_\gamma$) at the P2′ position in the inhibitors. In the models, both the cyclohexyl (**1e**, Figure 3A) and *tert*-butyl (**1f**, Figure 3B) inhibitors had a χ_1 value of about 60° (gauche +). This corresponds to one of the lowest-energy conformers. In contrast, the χ_1 value of the phenyl side chain of 1**a** was almost 0° (cis). Clearly this is an unstable conformer, but **1a** can not readjust its tertiary structure as Phe165 and Phe233 restrict rotation about the χ_1 dihedral (see Figure 3C). Simply stated, the **1a** conformer bound to MT1-MMP is not at an energy minimum, whereas **1e**,**f** can bind to MT1-MMP in their most stable form. This would be the reason for the selectivity between **1a**,**e**,**f**, and the narrow S2′ subsite of MT1-MMP would cause such a selectivity.

Looking at the S1′ subsite, MT1-MMP would be similar to MMP-2, -3, and -9, but not to MMP-1. MMP-1 has a characteristic arginine (Arg195) in its S1′ subsite (Figure 2). The long side chain of Arg195 extends to the bottom of the S1′ subsite and forms a rather shallow pocket (Figure 1). In other MMPs, this arginine is replaced by a leucine. The shorter side chain of the leucine would make the S1′ subsite deeper than that seen in MMP-1. Thus, a longer side chain at the P1′ position of the inhibitors would be preferable for these MMPs. Recently, Stams et al. have also elucidated this specificity resulting from the S1′ subsite.[14]

Conclusion

The present study elucidated structural activity profiles of hydroxamates affecting the selectivity toward ΔMT1. The P1′ 3-phenylpropyl group is preferable for binding to ΔMT1 and also MMP-2, -3, and -9. In addition, the shape of the P2′ substituent is critical in the binding of ΔMT1, and the S2′ subsite is narrower than those of other MMPs. Our molecular modeling study of ΔMT1 confirms this data. MT1-MMP restricts structural variance in its ligands by the characteristic phenylalanines at S2′ and S1 sites. Hence, it might be difficult to develop a specific inhibitor to MT1-MMP via the modification of P1′ and P2′ substituents of a pseudopeptide inhibitor. MMP-2, -3, or -9 accepts a wider range of ligands than MT1-MMP; an effective inhibitor to MT1-MMP might also bind to MMP-2, -3, or -9. However, an inhibitor that exhibits strong activity against both MT1-MMP and MMP-2 could have an advantage for the treatment of certain cancers. For the discovery of more specific inhibitors to MT1-MMP, further elucidation of the ligand−enzyme interaction by the enzyme and the design of non-peptide inhibitors based on the above information will be needed.

Experimental Section

Melting points were determined on a Buchi capillary melting point apparatus (model 535) and are uncorrected. ^{1}H NMR spectra were recorded on a Bruker AM300 spectrometer using TMS as an internal standard. Elemental analyses were performed on a Yanagimoto CHN-CORDER MT-3. Compounds **1a** and **2a**,**b** were prepared and characterized previously by us.[7] Compounds **2c** (BB-2516)[21] and **2d** (BB-94)[22] were synthesized according to the reported methods.

[4-(*N*-Hydroxyamino)-2(*R*)-(2-phenylethyl)succinyl]-L-phenylglycine-*N*-methylamide (1b). (i) 4(*S*)-Benzyl-2-oxazolidinone (5.0 g, 28.2 mmol) was dissolved in dry THF (50 mL) and cooled to −78 °C under a nitrogen atmosphere; 1.6 M *n*-BuLi in hexane (18 mL) was added dropwise with stirring while maintaining the temperature under −65 °C. The reaction mixture was stirred at −78 °C for 25 min, and a solution of 4-phenylbutanoyl chloride in THF (10 mL), which was prepared from 4-phenylbutanoic acid (5.0 g, 30.4 mmol) and thionyl chloride (15 mL), was added dropwise. The reaction mixture was stirred at −78 °C for 30 min and allowed to gradually warm to room temperature, and then the reaction was quenched with the addition of 0.5 N HCl and extracted with AcOEt. The organic layer was washed with water, saturated aqueous $NaHCO_3$, water, and brine successively and dried over $MgSO_4$. The solvent was evaporated in vacuo, and the residue was purified by column chromatography on silica gel (AcOEt/*n*-hexane = 1/3) to give 4(*S*)-benzyl-3-(4-phenylbutanoyl)-2-oxazolidinone (**5b**; 7.4 g, 81%) as an oil. **5b**: ^{1}H NMR ($CDCl_3$) δ 1.93−2.10 (2H, m), 2.87−3.09 (3H, m), 3.27 (1H, dd, J = 3.3, 13.3 Hz), 4.10−4.20 (2H, m), 4.59−4.68 (1H, m), 7.13−7.36 (10H, m).

(ii) To a solution of diisopropylamine (1.7 g, 16.8 mmol) in THF (30 mL) were added dropwise at −78 °C 1.6 M *n*-BuLi in *n*-hexane (10 mL) and then a solution of compound **5b** (5.0 g, 15.5 mmol) in dry THF (20 mL). The reaction mixture was stirred at −78 °C for 40 min, and *tert*-butyl bromoacetate (4.0 g, 20.5 mmol) was added. The reaction mixture was stirred overnight while slowly warming to room temperature. The reaction was quenched with the addition of 0.5 N HCl and extracted with AcOEt. The organic layer was washed with water and brine successively and dried over $MgSO_4$. The solvent was evaporated in vacuo, and the residue was purified by column chromatography on silica gel (AcOEt/*n*-hexane = 1/3) to give 4(*S*)-benzyl-3-[2(*R*)-[(*tert*-butoxycarbonyl)methyl]-4-phenylbutanoyl]-2-oxazolidinone (**6b**; 4.0 g, 59%). **6b**: ^{1}H NMR ($CDCl_3$) δ 1.43 (9H, s), 1.70−1.90 (1H, m), 2.53 (1H, dd, J = 4.5, 16.6 Hz), 2.62−2.77 (3H, m), 2.87 (1H, dd, J = 10.3, 16.6 Hz), 3.32 (1H, dd, J = 3.2, 13.4 Hz), 4.03−4.18 (2H, m), 4.20−4.33 (1H, m), 4.48−4.59 (1H, m), 7.1−7.4 (10H, m).

(iii) To a solution of **6b** (4.0 g, 9.1 mmol) in THF (100 mL) and water (30 mL) were added aqueous 30% H_2O_2 (4.5 mL) and LiOH monohydrate (650 mg, 15.5 mmol) in water (30 mL) below 5 °C, and the mixture was stirred at room temperature

for 1.5 h. The reaction mixture was cooled in an ice bath, and sodium nitrite (2.7 g) was added. After stirring for 30 min the THF was evaporated and the remaining water layer was washed with chloroform. The water layer was acidified with2 N HCl to pH 2−3 and extracted with AcOEt, and the extract was washed with water and brine and dried over $MgSO_4$. Evaporation of the solvent gave the acid **7b** (2.5 g, 98.2%) as an oil. **7b**: ^{1}H NMR ($CDCl_3$) δ 1.43 (9H, s), 1.8−1.9 (1H, m), 1.9−2.1 (1H, m), 2.44 (1H, dd, J = 5.2, 16.3 Hz), 2.6−2.8 (3H, m), 2.8−2.9 (1H, m), 7.1−7.3 (5H, m).

(iv) To a solution of L-phenylglycine-*N*-methylamide (476 mg, 2.9 mmol), HOBT (390 mg), and **7b** (800 mg, 2.9 mmol) in DMF (10 mL) was added 1-[3-(dimethylamino)propyl]-3-ethylcarbodiimide hydrochloride (556 mg, 2.9 mmol), and the mixture was stirred at room temperature overnight. The reaction mixture was diluted with AcOEt, washed with 0.5 N HCl, water, saturated aqueous $NaHCO_3$ solution, and brine successively, and dried over $MgSO_4$. After evaporation of the solvent, the obtained residue was purified by silica gel column chromatography (AcOEt/*n*-hexane = 1/1) to afford **8b** (0.84 g, 91.8%) as colorless crystals. **8b**: ^{1}H NMR ($CDCl_3$) δ 1.32 (9H, s), 1.6−1.8 (1H, m), 1.9−2.1 (1H, m), 2.33 (1H, dd, J = 4.8, 16.4 Hz), 2.5−2.8 (4H, m), 2.81 (3H, d, J = 4.9 Hz), 5.43 (1H, d, J = 6.9 Hz), 5.8−5.9 (1H, m), 7.0−7.4 (1H, m).

(v) A solution of **8b** (0.84 g, 1.98 mmol) in 90% aqueous TFA (3 mL) was stirred under ice cooling for 1 h. After the solvent was evaporated, the residue was dissolved in chloroform. The chloroform solution was washed with water and brine, dried over $MgSO_4$, and evaporated to give **9b** (0.58 g, 79.6%) as colorless crystals. **9b**: ^{1}H NMR (DMSO-d_6) δ 1.58−1.85 (2H, m), 2.30 (1H, dd, J = 5.5, 16.4 Hz), 2.44−2.70 (6H, m), 2.83−2.97 (1H, m), 5.43 (1H, d, J = 7.7 Hz), 7.10−7.44 (10H, m), 8.14−8.23 (1H, m), 8.47 (1H, d, J = 7.8 Hz), 12.0 (1H, bs).

(vi) To a solution of **9b** (580 mg, 1.57 mmol), HOBT monohydrate (281 mg, 1.9 mmol), and 1-[3-(dimethylamino)propyl]-3-ethylcarbodiimide hydrochloride (364 mg, 1.9 mmol) in DMF (10 mL) were added O-benzylhydroxylamine hydrochloride (303 mg, 1.9 mmol) and triethylamine (191 mg, 1.9 mmol), and the mixture was stirred at room temperature overnight. The reaction mixture was diluted with AcOEt, washed with 0.5 N HCl, water, saturated aqueous $NaHCO_3$ solution, and brine successively, and dried over $MgSO_4$. After evaporation of the solvent, the resultant syrup was purified with silica gel column chromatography (chloroform/MeOH = 200/1) to give compound **10b** (633 mg, 85%) as a syrup.

(vii) Compound **10b** (630 mg, 1.33 mmol) was hydrogenated in methanol (10 mL) with 10% Pd/C (80 mg) under hydrogen atmosphere (3 kg/cm^2) at room temperature. The catalyst was removed by filtration, and the filtrate was evaporated. The residue was crystallized from a mixture of methanol and AcOEt to give **1b** (300 mg, 59%) as colorless crystals.

1b: mp 191−194 °C; ^{1}H NMR (DMSO-d_6) δ 1.55−1.80 (2H, m), 2.06 (1H, dd, J = 7.5, 14.4 Hz), 2.23 (1H, dd, J = 7.0, 14.4 Hz), 2.40−2.70 (2H, m), 2.59 (3H, d, J = 4.4 Hz), 2.82−2.98 (1H, m), 5.41 (1H, d, J = 7.7 Hz), 7.10−7.50 (10H, m), 8.12−8.22 (1H, m), 8.49 (1H, d, J = 7.7 Hz), 8.73 (1H, s), 10.40 (1H, s). Anal. ($C_{21}H_{25}N_3O_4 \cdot 0.7H_2O$) C, H, N.

Compounds **1c**,**d**,**h**,**i** were obtained in a similar manner of preparation as for **1b**. Their physical data are summarized as follows.

[4-(*N*-Hydroxyamino)-2(*R*)-(3-phenylpropyl)succinyl]-L-phenylglycine-*N*-methylamide (1c): mp 176−179 °C; ^{1}H NMR (DMSO-d_6) δ 1.30−1.60 (4H, m), 1.99 (1H, dd, J = 7.2, 14.5 Hz), 2.17 (1H, dd, J = 7.1, 14.5 Hz), 2.45−2.65 (2H, m), 2.56 (3H, d, J = 4.4 Hz), 2.80−2.93 (1H, m), 5.39 (1H, d, J = 7.8 Hz), 7.10−7.43 (10H, m), 8.08-8.20 (1H, m), 8.46 (1H, d, J = 7.8 Hz), 8.71 (1H, s), 10.36 (1H, s). Anal. ($C_{22}H_{27}N_3O_4$) C, H, N.

[4-(*N*-Hydroxyamino)-2(*R*)-nonylsuccinyl]-L-phenylglycine-*N*-methylamide (1d): ^{1}H NMR (DMSO-d_6) δ 0.63 (3H, t, J = 6.8 Hz), 0.9−1.3 (16H, m), 1.74 (1H, dd, J = 7.5, 14.7 Hz), 1.92 (1H, dd, J = 7.0, 14.7 Hz), 2.34 (3H, d, J = 4.5 Hz), 2.50−2.65 (1H, m), 5.15 (1H, d, J = 7.9 Hz), 7.00−7.20 (5H, m), 7.85−7.95 (1H, m), 8.19 (1H, d, J = 7.9 Hz), 8.46 (1H, s), 10.11 (1H, s). Anal. ($C_{22}H_{35}N_3O_4$) C, H, N.

[4-(*N*-Hydroxyamino)-2(*R*)-(3-phenylpropyl)succinyl]-L-*tert*-butylglycine-*N*-methylamide (1h): mp 184−185 °C dec; ^{1}H NMR (DMSO-d_6) δ 0.70 (9H, s), 1.10−1.35 (4H, m), 1.84 (1H, dd, J = 14.5, 6.5 Hz), 2.00 (1H, dd, J = 14.5, 6.5 Hz), 2.35 (3H, d, J = 4.5 Hz), 2.55−2.75 (1H, m), 3.97 (1H, d, J = 9.5 Hz), 6.90−7.10 (5H, m), 7.39 (1H, br), 7.57 (1H, br), 8.39 (1H, br), 10.08 (1H, bs). Anal. ($C_{20}H_{31}N_3O_4 \cdot {}^1/_4H_2O$) C, H, N.

[4-(*N*-Hydroxyamino)-2(*R*)-(3-phenylpropyl)succinyl]-L-valine-*N*-methylamide (1i): mp 180−185 °C dec; ^{1}H NMR (DMSO-d_6) δ 0.85 (6H, d, J = 6.6 Hz), 1.3−1.6 (4H, m), 1.9−2.1 (2H, m), 2.17 (1H, dd, J = 7.2, 14.5 Hz), 2.5−2.55 (2H, m), 2.58 (3H, d, J = 4.5 Hz), 2.74−2.77 (1H, m), 4.06−4.12 (1H, m), 7.0−7.36 (5H, m), 7.64 (2H, br), 8.16 (1H, s), 10.36 (1H, s). Anal. ($C_{19}H_{29}N_3O_4$) C, H, N.

[4-(*N*-Hydroxyamino)-2(*R*)-isobutylsuccinyl]-L-cyclohexylglycine-*N*-methylamide (1e). (i) To a solution of L-phenylglycine-*N*-methylamide[7] (1.15 g, 7 mmol) in ethanol (50 mL) was added rhodium chloride trihydrate (3 g), and the mixture was stirred at 30 °C for 2 h. Then a solution of sodium borohydride (2.5 g, 66 mmol) in ethanol (100 mL) was added to the mixture dropwise for 35 min, and the mixture was stirred at room temperature for 4 h. After removal of insoluble material by filtration, the filtrate was evaporated in vacuo. The obtained residue was dissolved in 1 N HCl, washed with AcOEt, neutralized by sodium carbonate, and extracted with AcOEt. The organic layer was dried over $MgSO_4$ and evaporated in vacuo to give L-cyclohexylglycine-*N*-methylamide as a crude syrup (700 mg, 58.7%).

(ii) To a solution of L-cyclohexylglycine-*N*-methylamide (444 mg, 2.6 mmol) and 4-[*N*-(benzyloxy)amino]-2(*R*)-isobutylsuccinic acid[7] (**1**; 730 mg, 2.6 mmol) in DMF (20 mL) was added 1-ethyl-3-[3-(dimethylamino)propyl]carbodiimide hydrochloride (750 mg, 3.9 mmol), and the mixture was stirred at room temperature overnight. The precipitate was collected by filtration and washed with AcOEt to give compound **4e** (725 mg, 64.6%) as colorless crystals. Hydrogenation of **4e** in methanol with 10% Pd/C and recrystallization from AcOEt−MeOH afforded **1e** (290 mg, 50.6%) as colorless crystals. **1e:** mp 215 °C dec; ^{1}H NMR (DMSO-d_6) δ 0.79 (3H, d, J = 6.2 Hz), 0.83 (3H, d, J = 6.2 Hz), 0.8−1.23 (6H, m), 1.33−1.72 (8H, m), 1.99 (1H, dd, J = 7.7, 14.3 Hz), 2.14 (1H, dd, J = 6.4, 14.3 Hz), 2.55 (3H, d, J = 4.5 Hz), 2.70−2.82 (1H, m), 4.03 (1H, t, J = 8.1 Hz), 7.73−7.83 (2H, m), 8.71 (1H, s), 10.37 (1H, s). Anal. ($C_{17}H_{31}N_3O_4$) C, H, N.

[4-(*N*-Hydroxyamino)-2(*R*)-isobutyl-3(*S*)-methylsuccinyl]-L-cyclohexylglycine-*N*-methylamide (2f). (i) To a solution of benzyl 2-[(benzyloxy)carbonyl]-3(*R*)-(hydroxycarbonyl)-5-methylhexanoate[7] (**13**; 4.4 g, 11 mmol) in DMF (20 mL) were added L-cyclohexylglycine-*N*-methylamide (1.9 g, 11.2 mmol), HOBT monohydrate (1.5 g), and 1-[3-(dimethylamino)propyl]-3-ethylcarbodiimide hydrochloride (2.1 g, 11 mmol) with ice cooling, and the mixture was stirred at room temperature overnight. To the reaction mixture was added 0.5 N HCl, and the mixture was extracted with EtOAc (100 mL). The organic layer was washed with water, 0.5 N HCl, saturated aqueous $NaHCO_3$ solution, and brine successively. After drying over anhydrous $MgSO_4$, the organic solution was evaporated in vacuo. The obtained residue was purified with silica gel column chromatography (chloroform/MeOH = 20/1) to give **14f** (3.0 g, 50%) as a syrup.

14f: ^{1}H NMR ($CDCl_3$) δ 0.75−0.85 (6H, m), 0.8−1.9 (14H, m), 2.7−2.8 (3H, m), 2.9−3.1 (1H, m), 3.80 (1H, d), 4.1−4.2 (1H, m), 5.0−5.2 (4H, m), 6.1−6.2 (1H, m), 6.5−6.6 (1H, d), 7.2−7.4 (10H, m).

(ii) Compound **14f** (3.0 g, 5.4 mmol) was hydrogenated in EtOH (30 mL) with 10% Pd/C (0.2 g) under hydrogen atmosphere at room temperature for 4 h. After removal of the catalyst by filtration, piperidine (0.57 g, 6.7 mmol) and 37% aqueous formaldehyde solution (2.5 mL) were added, and the mixture was stirred at room temperature for 16 h and then refluxed for 1 h. The solvents were removed under reduced

pressure, and the residue was partitioned between 10% aqueous citric acid solution (50 mL) and EtOAc (50 mL). The acid layer was extracted with EtOAc (40 mL × 2). The organic layer was combined and extracted with 10% aqueous potassium carbonate solution (40 mL × 3).

These aqueous extracts were acidified to pH 4 with 2 N HCl and extracted with EtOAc (50 mL × 2). The EtOAc extracts were dried over $MgSO_4$ and evaporated in vacuo to give **15f** (1.4 g, 76%) as a white solid. **15f**: ^{1}H NMR ($CDCl_3$ + DMSO-d_6) δ 0.86 (3H, d, J = 6.2 Hz), 0.90 (3H, d, J = 6.2 Hz), 0.8−1.8 (14H, m), 2.70 (3H, d, J = 4.6 Hz), 3.5−3.7 (1H, m), 4.18 (1H, t, J = 7.4 Hz), 5.76 (1H, s), 6.29 (1H, s), 7.25 (1H, br), 7.66 (1H, br).

(iii) Compound **15f** (1.4 g, 4.1 mmol) was hydrogenated in methanol (30 mL) with 10% Pd/C (300 mg) under hydrogen atmosphere at room temperature. The catalyst was removed by filtration, and the filtrate was evaporated to give **16f** as a syrup. To a solution of **16f** (1.4 g, 4.1 mmol), HOBT monohydrate (0.66 g), and 1-[3-(dimethylamino)propyl]-3-ethylcarbodiimide hydrochloride (0.95 mg, 5 mmol) in DMF (30 mL) were added *O*-benzylhydroxylamine hydrochloride (790 mg, 5 mmol) and triethylamine (0.5 g, 5 mmol), and the mixture was stirred at room temperature overnight for 12 h. The precipitated solid was collected by filtration and washed with cold ethanol to give **17f** (1.1 g, 59%) as colorless crystals. Compound **17f** (1.1 g, 2.4 mmol) was hydrogenated in methanol (30 mL) and THF (30 mL) with 10% Pd/C (0.2 g) under hydrogen atmosphere at room temperature. The catalyst was removed by filtration, and the filtrate was evaporated. The residue was crystallized from methanol to give **2f** (437 mg, 50%) as colorless crystals. **2f:** ^{1}H NMR (DMSO-d_6) δ 0.75 (3H, d, J = 6.4 Hz), 0.81 (3H, d, J = 6.4 Hz), 0.91 (3H, d, J = 6.8 Hz), 0.7−1.8 (14H, m), 2.0−2.2 (1H, m), 2.4−2.6 (1H, m), 2.55 (3H, d, J = 4.5 Hz), 4.03 (1H, t, J = 8.4 Hz), 7.6−7.7 (1H, m), 8.03 (1H, d, J = 8.4 Hz), 8.76 (1H, s), 10.45 (1H, s). Anal. ($C_{18}H_{33}N_3O_4$) C, H, N.

[4-(*N*-Hydroxyamino)-2(*R*)-isopropyl-3(*S*)-methylsuccinyl]-L-3-(5,6,7,8-tetrahydro-1-naphthyl)alanine-*N*-methylamide (2e). Hydrogenation of [4-[*N*-(benzyloxy)amino]-2 (*R*)-isopropyl-3(*S*)-methylsuccinyl]-L-3-(5,6,7,8-tetrahydro-1-naphthyl)alanine-*N*-methylamide (**17e**; 500 mg, 1 mmol), which was obtained in a similar manner as for preparation of **17f**, with 10% Pd/C (150 mg) in acetic acid (20 mL) at 4 kg/m^2 hydrogen pressure for 40 h and recrystallization from methanol afforded **2e** (210 mg, 50.7%) as colorless crystals. **2e:** mp 223−224 °C dec; ^{1}H NMR (DMSO-d_6) δ 0.59 (3H, d, J = 6.7 Hz), 0.74 (3H, d, J = 6.4 Hz), 0.80 (3H, d, J = 6.4 Hz), 0.8−0.9 (1H, m), 1.2−1.45 (2H, m), 1.6−1.85 (4H, m), 1.95−2.1 (1H, m), 2.3−2.5 (1H, m), 2.54 (3H, d, J = 4.6 Hz), 2.6−2.95 (6H, m), 4.45−4.6 (1H, m), 6.8−7.05 (3H, m), 7.67 (1H, q, J = 4.6 Hz), 8.25 (1H, d, J = 8.6 Hz), 8.72 (1H, s), 10.39 (1H, s). Anal. ($C_{23}H_{35}N_3O_4$) C, H, N.

MMP Inhibition Assay. ΔMT1 was purified according to the methods reported by Ohuchi et al.[5] The inhibitory activity of the test compound to ΔMT1 was determined by using the synthetic peptide substrate, the coumarinyl peptide derivative Mca-Pro-Leu-Gly-Dpa-Ala-Arg-NH_2 (Peptide Institute, Inc., Osaka, Japan). Mixture of ΔMT1 (0.5 nM) and various concentrations of the compounds in 400 μL of 50 mM Tris-HCl buffer (pH 7.5), 0.15 M NaCl, 10 mM $CaCl_2$, 0.05% Brij-35, and 0.02% NaN_3 was incubated at 37 °C for 1 h and then reacted with 100 μL of the substrate (a final concentration of 1 μM) for 1 h at 37 °C. The emergence of fluorescence intensity (ex 328 nm, em 393 nm) was measured after termination of the reaction with 2500 μL of 0.1 M sodium acetate buffer (pH 4.0). Percent inhibition of the substrate was calculated from the difference of fluorescence intensity between the presence and absence of the compounds.

MMP-1 and -9 inhibitory activities by the synthetic compounds were measured by the methods reported previously.[7]

MMP-2 inhibitory activity was determined by the modified method of Nagai et al.[24] using a fluorescent isothiocyanate (FITC)-labeled gelatin, which was prepared by denaturing FITC-labeled collagen at 60 °C for 30 min, as substrate. ProMMP-2 was purified from culture medium of human glioblastoma cell line T98G (ATCC CRL 1690) by a similar method in the literature.[25] MMP-2 was prepared by activating proMMP-2 with 1 mM (4-aminophenyl)mercuric acetate at 37 °C for 2 h, and 1 unit of MMP-2 was defined as the amount of the enzyme required to degrade 1 μg of FITC-gelatin in 1 min at 37 °C. For MMP-2 inhibition assay, activated MMP-2 (50 μL, 0.013 U) and FITC-labeled gelatin (250 μg/mL) were incubated in 50 mM Tris-HCl buffer (pH 7.5) containing 0.2 M NaCl, 5 mM $CaCl_2$, and 0.05% Brij-35 at 35 °C for 16−18 h. The reaction was terminated by the addition of 200 μL of cold 22% trichloroacetic acid. The mixture was vortexed and centrifuged at 10 000 rpm for 6 min, and to 300 μL of the supernatant was added 100 μL of a buffer containing 5.5 volumes of 1.5 M Tris-HCl (pH 8.8), 3.3 volumes of 10 M NaOH, and 8 volumes of water. Then, fluorescence intensity (ex 495 nm, em 520 nm) of the mixture was measured. Percent inhibition of gelatin degradation was calculated from the difference of fluorescence intensity between the presence and absence of test compounds. The IC_{50} was calculated from a least-squares fit of the percent inhibition and inhibitor concentration.

MMP-3 inhibitory activity was determined by the modified method of Nagase and Woessner[26] using a radiolabeled proteoglycan substrate entrapped in polyacrylamide particles. The radiolabeled proteoglycan substrate was prepared according to the method reported by Hascall[27] and Montelaro.[28] MMP-3 was purified from culture medium of human fibroblasts by the methods of Okada et al., and 1 unit was defined as the amount of enzyme required to catalyze the production of 1 mg of carboxymethylated transferrin fragments soluble in 3.3% trichloroacetic acid in 1 min at 37 °C.[29] For enzyme inhibition assay, 0.3 U/mL MMP-3 and 3.5 mg of dry beads were used, and IC_{50} values were obtained from dose-dependent inhibition curves.

References

(1) For review: *Inhibition of Matrix Metalloproteinases*; Greenwald, R. A., Golub, L. M., Eds.; The New York Academy of Sciences: New York, 1994; Vol. 732.

(2) Stetler-Stevenson, W. G.; Aznavoorian, S.; Liotta, L A. Tumor cell interactions with extracellular matrix during invasion and metastasis. *Annu. Rev. Cell Biol.* **1993**, *9*, 541−573.

(3) Nagase, H.; Enghild, J. J.; Suzuki, K.; Salvensen, G. Stepwise activation mechanism of the precursor of matrix metalloproteinase 3 (stromelysin) by proteinases and (4-aminophenyl)-mercuric acetate. *Biochemistry* **1990**, *29*, 5783−5789.

(4) Sato, H.; Takino, T.; Okada, Y.; Cao, J.; Shinagawa, A.; Yamamoto, Y.; Seiki, M. A matrix metalloproteinase expressed on the surface of invasive tumor cells. *Nature* **1994**, *370*, 61−65.

(5) (a) Nomura, H.; Sato, H.; Seiki, M.; Mai, M.; Okada, Y. Expression of membrane-type matrix metalloproteinase in human gastric carcinomas. *Cancer Res.* **1995**, *55*, 3263−3266. (b) Ueno, H.; Nakamura, H.; Inoue, M.; Imai, K.; Noguchi, M.; Satoh, H.; Seiki, M.; Okada, Y. Expression and tissue localization of membrane-types 1, 2 and 3 matrix metalloproteinases in human invasive breast carcinomas. *Cancer Res.* **1997**, *57*, 2055−2060.

(6) Ohuchi, E.; Imai, K.; Fujii, Y.; Sato, H.; Seiki, M.; Okada, Y. Membrane type 1 matrix metalloproteinase digests interstitial collagens and other extracellular matrix macromolecules. *J. Biol. Chem.* **1997**, *272*, 2446−2451.

(7) Hirayama, R.; Yamamoto, M.; Tsukida, T.; Matsuo, K.; Obata, Y.; Sakamoto, F.; Ikeda, S. Synthesis and biological evaluation of orally active matrix metalloproteinase inhibitors. *Bioorg. Med. Chem.* **1997**, *5*, 765−778.

(8) Wech, A. R.; Holman, C. M.; Huber, M.; Brenner, M. C.; Browner, M. F.; Van Wart, H. E. Understanding the P1′ specificity of the matrix metalloproteinases: Effect of S1′ pocket mutation in matrilysin and stromelysin-1. *Biochemistry* **1996**, *35*, 10103−10109.

(9) Miller, A.; Askew, M.; Beckett, R. P.; Bellamy, C. L.; Bone, E. A.; Coates, R. E.; Davidson, A. H.; Drummond, A. H.; Huxley, P.; Martin, F. M.; Saroglou, M. L.; Thompson, A. J.; van Dijk, S. E.; Whittaker, M. Inhibition of matrix metalloproteinases: An examination of the S1′ pocket. *Bioorg. Med. Chem. Lett.* **1997**, *7*, 193−198.

(10) (a) Strongin, A. Y.; Marmer, B. L.; Grant, G. A.; Goldberg, G. I. Plasma membrane-dependent activation of the 72-kDa type IV collagenase is prevented by complex formation with TIMP-2. *J. Biol. Chem.* **1993**, *268*, 14033−14039. (b) Atkinson, S. J.;

Crabbet, T.; Cowell, S.; Ward, R. V.; Butlet, M. J.; Sato, H.; Seiki, M.; Reynold, J. J.; Murphy, G. Intermolecular autolytic cleavage can contribute to the activation of progelatinase A by cell membranes. *J. Biol. Chem.* **1995**, *270*, 30479−30485.
(11) Beckett, R. P.; Davidson, A. H.; Drummond, A. H.; Huxley, P.; Whittaker, M. Recent advances in matrix metalloproteinase inhibitor research. *Drug Discovery Today* **1996**, *1*, 16−26.
(12) Peitsch, M. C. Protein modeling by E-mail. *Bio/Technology* **1995**, *13*, 658−660.
(13) Peitsch, M. C. ProMod and Swiss-Model: Internet-based tools for automated comparative protein modelling. *Biochem. Soc. Trans.* **1996**, *24*, 274−279.
(14) Stams, T.; Spurlino, J. C.; Smith, D. L.; Wahl, R. C.; Ho, T. F.; Qoronfleh, M. W.; Banks, T. M.; Rubin, B. Structure of human neutrophil collagenase reveals large S1′ specificity pocket. *Nature Struct. Biol.* **1994**, *1*, 119−123.
(15) Grams, F.; Crimmin, M.; Hinnes, L.; Huxley, P.; Pieper, M.; Tschesche, H.; Bode, W. Structure determination and analysis of human neutrophil collagenase complexed with a hydroxamate inhibitor. *Biochemistry* **1995**, *34*, 14012−14020.
(16) Bode, W.; Reinemer, P.; Huber, R.; Kleine, T.; Schnierer, S.; Tschesche, H. The X-ray crystal structure of the catalytic domain of human neutrophil collagenase inhibited by a substrate analogue reveals the essentials for catalysis and specificity. *EMBO J.* **1994**, *13*, 1263−1269.
(17) Browner, M. F.; Smith, W. W.; Castelhano, A. L. Matrilysin−inhibitor complexes: Common themes among metalloproteases. *Biochemistry* **1995**, *34*, 6602−6610.
(18) Spurlino, J. C.; Smallwood, A. M.; Carlton, D. D.; Banks, T. M.; Vavra, K. J.; Johnson, J. S.; Cook, E. R.; Falvo, J.; Wahl, R. C.; Pulvino, T. A.; Wendoloski, J. J.; Smith, D. L. 1.56 Å structure of mature truncated human fibroblast collagenase. *Proteins Struct. Funct. Genet.* **1994**, *19*, 98−109.
(19) Lovejoy, B.; Hassell, A. M.; Luther, M. A.; Weigl, D.; Jordan, S. R. Crystal structures of recombinant 19-kDa human fibroblast collagenase complexed to itself. *Biochemistry* **l994**, *33*, 8207−8217.
(20) Galardy, R. E. *Drugs Future* **1993**, *18*, 1109−1111.
(21) *(*21) Dickens, J. P.; Crimmin, M. J.; Beckett, R. P. PCT Patent Application WO9402447, 1994.
(22) Campion, C.; Davidson, A. H.; Dickens, J. P.; Crimmin, M. J. PCT Patent Application WO9005719, 1990.
(23) Handa, B. K.; Johnson, W. H.; Machin, P. J. Eur. Patent Application EP 236872, 1987.
(24) Nagai, N.; Hori, H.; Hattori, S.; Sunada, Y.; Terada, K.; Hashida, R.; Miyamoto, K. A micro-assay method of collagenase activity and its application in the study of collagen metabolism in pathological tissues. *Jpn. J. Inflamm.* **1984**, *4*, 123−130.
(25) (a) Terato, K.; Hashida, R.; Miyamoto, K.; Morimoto, T.; Kato, Y.; Kobayashi, S.; Tajima, T.; Otake, S.; Hori, H.; Nagai, Y. Histological, immunological and biochemical studies on type II collagen-induced arthritis in rats. *Biomed. Res.* **1982**, *3*, 495−505. (b) Yasumitsu, H.; Miyazaki, K.; Umenishi, F.; Koshikawa, N.; Umeda, M. Comparison of extracellular matrix-degrading activities between 64-kDa and 90-kDa gelatinases purifies in inhibitor-free forms from human schwannoma cells. *J. Biochem.* **1992**, *111*, 74−80. (c) Howard, E. W.; Bullen, E. C.; Banda, M. J. Regulation of the autoactivation of human 72-kDa progelatinase by tissue inhibitor of metalloproteinase-2. *J. Biol. Chem.* **1991**, *266*, 13064−13069.
(26) Nagase, H.; Woessner, J. F. An improved assay for proteases and polysaccharidases employing a cartilage proteoglycan substrate entrapped in polyacrylamide particles. *Anal. Biochem.* **1980**, *107*, 385−392.
(27) Hascall, V. C.; Sajdera, S. W. Proteinpolysaccharide complex from bovine nasal cartilage. *J. Biol. Chem.* **1969**, *244*, 2384−2396.
(28) Montelaro, R. C.; Rueckert, R. R. Radiolabeling of proteins and viruses in vitro by acetylation with radioactive acetic anhydride. *J. Biol. Chem.* **1975**, *250*, 1413−1421.
(29) Okada, Y.; Nagase, H.; Harris, E. D., Jr. A metalloproteinase from human rheumatoid synovial fibroblasts that digests connective tissue matrix components. *J. Biol. Chem.* **1986**, *261*, 14245−14255.
(30) Sato, H.; Seiki, M. Membrane-type matrix metalloproteinases (MT-MMPs) in tumor metastasis. *J. Biochem.* **1996**, *119*, 209−215.

JM970404A